The International Journal of Artificial Organs / Vol. 31 / no. 6, 2008 / pp.

Regenerative Medicine

Human adipose-derived stem cells as future tools in tissue regeneration: Osteogenic differentiation and cell-scaffold interaction

L. DE GIROLAMO[1,2], M. F. SARTORI[1], E. ARRIGONI[1], L. RIMONDINI[3], W. ALBISETTI[4], R. L. WEINSTEIN[5], A. T. BRINI[1]

[1] Department of Medical Pharmacology, Faculty of Medicine, University of Milan, Milan - Italy
[2] IRCCS Galeazzi Orthopedic Institute, Milan - Italy
[3] University of Eastern Piedmont "A. Avogadro", Novara - Italy
[4] Orthopedic and Traumatology Institute, University of Milan, G. Pini Orthopedic Institute, Milan - Italy
[5] Department of Stomatology, University of Milan, IRCCS Galeazzi Orthopedic Institute, Milan - Italy

ABSTRACT: Tissue engineering is now contributing to new developments in several clinical fields, and mesenchymal stem cells derived from adipose tissue (hASCs) may provide a novel opportunity to replace, repair and promote the regeneration of diseased or damaged musculoskeletal tissue. Our interest was to characterize and differentiate hASCs isolated from twenty-three donors. Proliferation, CFU-F, cytofluorimetric and histochemistry analyses were performed. HASCs differentiate into osteogenic, chondrogenic, and adipogenic lineages, as assessed by tissue-specific markers such as alkaline phosphatase, osteopontin expression and deposition of calcium matrix, lipid-vacuoles formation and Glycosaminoglycans production. We also compared osteo-differentiated hASCs cultured on monolayer and loaded on biomaterials routinely used in the clinic, such as hydroxyapatite, cancellous human bone fragments, deproteinized bovine bone granules, and titanium. Scaffolds loaded with pre-differentiated hASCs do not affect cell proliferation and no cellular toxicity was observed. HASCs tightly adhere to scaffolds and differentiated-hASCs on human bone fragments and bovine bone granules produced, respectively, 3.4- and 2.1-fold more calcified matrix than osteo-differentiated hASCs on monolayer. Moreover, both human and deproteinized bovine bone is able to induce osteogenic differentiation of CTRL-hASCs. Although our in vitro results need to be confirmed in in vivo bone regeneration models, our data suggest that hASCs may be considered suitable biological tools for the screening of innovative scaffolds that would be useful in tissue engineering. (Int J Artif Organs 2008; 31:)

KEY WORDS: hASCs (human Adipose Stem Cells), Osteogenic differentiation, Scaffolds, Bone regeneration

INTRODUCTION

A promising way to promote tissue regeneration includes the use of constructs to be inserted in the defect site, using techniques developed by tissue engineering. These constructs may be generated with autologous cells, either terminally differentiated or undifferentiated, and loaded on suitable natural or synthetic scaffolds.

Recently, the interest in Mesenchymal Stem Cells (MSCs) for musculoskeletal tissue regeneration has significantly increased due to their wide characterization, their confirmed multipotential ability, and their availability (1, 2). Indeed, many *in vitro* and *in vivo* studies have shown the use of MSCs in the regeneration of bone and cartilage defects (3-7). Although bone marrow represents the most common source of MSC (Bone Marrow derived Stromal

0391-3988/001-13 $25.00/0

Cells - BMSC), several studies have indicated their presence in other tissues such as periostium, skeletal muscle, trabecular bone, synovial membrane and adipose tissue (8-10). It has been previously shown that human Adipose-derived Stem Cells (hASCs) are able to differentiate *in vitro* into bone, cartilage, fat, muscle, endothelial and neuronal-like cells (11-16), and since they can be easily isolated from lipoaspirated tissue (14), their use in research and for clinical applications may have several advantages. Furthermore, adipose tissue derived from the minimally invasive procedure of liposuction is usually discarded, and it has been shown that a significant number of hASCs can be isolated from a few milliliters of raw tissue. Moreover, they do not lose their proliferation rate and differentiation potential after cryopreservation (17). In addition, as several authors have reported regarding stromal cells derived from BMSC, these types of cells, isolated from the Stromal Vascular Fraction, are not negatively affected by the age of the donor (18,19).

In this study, we describe the mesenchymal immunophenotype of hASCs and their *in vitro* osteogenic and chondrogenic ability. In particular, we analyze the influence of a three-dimensional environment used for culturing hASCs, both differentiated and undifferentiated, on natural or synthetic scaffolds, which are used in orthopedic and dental applications.

MATERIALS AND METHODS

Materials and antibodies

All materials and tissue culture reagents were purchased from Sigma-Aldrich (Milan, Italy), unless otherwise stated, and type I collagenase was purchased from Worthington (Lakewood, NJ, USA). Antibodies used in flow cytometry and immunofluorescence experiments are shown in Table I.

Isolation and culture expansion of Human Adipose tissue-derived Stem Cells (hASCs)

Subcutaneous fat aspirates were obtained from 23 donors (mean age 38 years, range 21-60 years, BMI 22-40, 85% female), after written consent and Institutional Review Board (IRB) approval. Primary cultures of the stromal vascular fraction (SVF) were established as previously described (11). Briefly, the matrix was digested with 0.075% type I collagenase in a shaking water bath at 37°C for 30 minutes and then centrifuged for 10 minutes at 1200 g to separate the SVF from adipocytes, cellular debris and undigested tissue. Cells derived from the SVF were plated in control medium (media composition is listed in Table II), at 10^5 cells/cm^2. The cells were maintained at 37°C in a humidified atmo-

TABLE I - ANTIBODIES RAISED AGAINST HUMAN EPITOPES USED IN EXPERIMENTS OF FLOW CYTOMETRY AND IMMUNOFLUORESCENCE

Primary Antibody	Clone	Conjug.	Supplier
mAb anti-CD 13	22A5	FITC	Ancell (Bayport, MN, USA)
mAb anti-CD 14	UCHM1	FITC	"
mAb anti-CD 45	C11	FITC	"
mAb anti-CD 29	4B7R	biotin	"
mAb anti-CD 34	43A1	biotin	"
mAb anti-CD 49d	BU49	biotin	"
mAb anti-CD 54	15.2	biotin	"
mAb anti-CD 71	DF1513	biotin	"
mAb anti-CD 105	N1-3A1	biotin	"
mAb anti-CD 44	SFF-2	FITC	Alexis Biochemicals (San Diego, CA, USA)
mAb anti-CD 90	90C03	purified	Lab Vision (Fremont, CA, USA)
mAb anti-α-tubulin	DM1A	purified	Sigma-Aldrich (Milan, Italy)
rbAb anti-actin	A2066	purified	"
rbAb anti-osteopontin	RB-9097	purified	Lab Vision (Fremont, CA, USA)
mAb anti-collagen II	2B1.5	purified	"
Secondary detector		**Conjug.**	**Supplier**
streptavidin		R-PE	Ancell (Bayport, MN, USA)
sheep anti-mouse IgG antibody		FITC	Boeringher (Mannheim, Germany)
goat anti-rabbit IgG antibody		TRITC	Jackson Immunores. (West Grove, PA, USA)

sphere with 5% CO_2. After 24 to 48 hours, nonadherent cells were discarded and the medium was changed twice a week. Once they reached 80% of confluence, cells were detached by means of trypsin/EDTA (0.5% trypsin/0.2% EDTA) and plated at a density of 10^4 cells/cm^2 for further expansion.

Flow cytometry and immunofluorescence analysis

HASCs ($3X10^5$ per sample) were washed in PBS/10% FBS/0.01% NaN_3 and incubated with mAbs raised against CD13, CD14, CD29, CD34, CD44, CD45, CD49d, CD54, CD71, CD90 and CD105 (see Tab. I) for 30 minutes on ice. Primary antibodies were revealed either with Streptavidin-PE or FITC conjugated sheep anti-mouse Ab for 20 minutes at 4°C. Samples were analyzed using FACS (FACSCalibur flowcytometer - BD Biosciences Europe, Erembodegem, Belgium) and data was analyzed using CellQuest software (BD Biosciences Europe).

Fibroblast – Colony Forming Unit (CFU-F) assay

The CFU-F assay was performed as previously described (20), with minor modifications. HASCs were plated by limiting dilution in 6-well plates (from 48 cell/cm^2 to 1 cell/cm^2) and cultured in DMEM/20% FBS. At day 6, the medium was changed, and at day 10, cells were fixed with methanol and stained with 0.5% Crystal Violet. The frequency of the CFU-F was established by scoring individual colonies with respect to the number of seeded cells.

Cell lineage differentiation and evaluation of differentiation markers

Osteogenic differentiation

At passage 4, hASCs were plated at 10^4 hASC/cm^2 in control and osteogenic induction medium (Tab. II), replacing the medium twice a week. At day 7, 14, and 21 of the culture, cells were lysed (Triton X-100 0.1% in ddH_2O) and intracellular alkaline phosphatase activity (ALP) was measured. Cell lysates were incubated at 37°C in the presence of 1 mM p-nitrophenylphosphate (pNPP) in alkaline buffer (100 mM diethanolamine and 0.5 mM $MgCl_2$, pH 10.5) (21). The reaction was stopped with NaOH 1 N and samples read at 410 nm with the Wallac Victor II plate reader (Perkin Elmer Western Europe, Monza, Italy). Total protein content was determined by BCA Protein Assay (Pierce Biotechnology, Rockford, IL, USA).

To evaluate calcium deposition, 10^4 hASC/cm^2 were cultured in control and osteogenic media without any cell detachment for 14 to 21 days. Wells were rinsed with PBS and fixed with ice-cold 70% ethanol for 1 hour. Samples were then stained with 40 mM Alizarin Red-S (ARS) (pH 4.1) for 15 minutes and rinsed with distilled H_2O. Each sample was then incubated with 10% w/v cetylpyridinium chloride (CPC) in 0.1M phosphate buffer (pH 7.0) for 30 minutes to extract the stained matrix and read at 550 nm (22) with the Wallac Victor II plate reader.

Osteopontin expression was assessed by immunofluorescence experiments: cells cultured on coverslips for 14 days were fixed in 3% paraformaldheyde, permeabilized for 4 minutes in PBS/0.1% Triton X-100 and then incubated with a rabbit anti-human osteopontin Ab and a mouse anti-human α-tubulin mAb for 60 minutes at RT. The

TABLE II - LINEAGE SPECIFIC DIFFERENTIATION MEDIA

Medium	Media	Serum	Supplementation
Control (CTRL)	DMEM	10% FBS	none
Adipogenic			
- induction	DMEM	10% FBS	1µM dexamethasone, 10 µg/mL insulin, 500 µM IBMX (3-isobutyl-1-methyl-xanthine), 200 µM indomethacin
- maintenance	DMEM	10% FBS	10 µg/mL insulin
Osteogenic	DMEM	10% FBS	10 nM dexamethasone, 10 mM glicerol-2-phosphate, 150 µM L-ascorbic acid-2-phosphate, 10nM cholecalciferol
Chondrogenic	DMEM	1% FBS	100 nM dexamethasone, 110 mg/L sodium pyruvate, 150 µM L-ascorbic acid-2-phosphate, 1X ITS, 10 ng/mL TGF-β1[1]

[1] Invitrogen-BioSource (Camarillo, CA, USA)

primary antibodies were revealed with a TRITC conjugated goat anti-rabbit IgG and a FITC conjugated sheep anti-mouse IgG for 30 minutes at RT.

Chondrogenic differentiation

Chondrogenic differentiation was obtained either in monolayer or in pellet culture conditions: $5X10^5$ hASCs were centrifuged (500 g, 3 min) in a 15 mL centrifuge tube, the pellets were resuspended in control or chondrogenic induction media (see Tab. II) and then re-centrifuged (500 g, 3 min); media were changed twice a week. After 21 to 28 days, pellets were fixed in 10% neutral buffered formalin, dehydrated with a series of graded ethanol, embedded in paraffin and cut into 10 µm thick sections. Micromass sections were stained with hematoxylin/eosin or Alcian Blue 8GX; briefly, sections were stained with Alcian Blue solution (1% w/v in 3% glacial acetic acid, pH2.5) and counterstained with nuclear fast red (0.1% w/v).

Cells grown on monolayer were also stained with Alcian Blue as described above. Alcian Blue dye deposition was quantified by acquiring digital images with specialized image analysis software. Deposition was expressed as the brightness value of several randomly chosen areas (n=9) of the cellular soma. For sulfated glycosamminglycans (GAGs), quantification micromasses of 21 days in culture were digested by proteinase K (50 µg/mL in 100 mM K2HPO4, pH 8.0) at 56°C, according to a modified version of the dimethylmethylene blue (DMMB) assay (23). GAGs content were expressed as µg/pellet using bovine trachea chondroitin-4-sulfate (0 to 8 µg/mL) as standard. Immunofluorescence experiments were performed to evaluate collagen II expression: 21 days differentiated cells grown in monolayer were allowed to adhere on coverslips for three days, then processed as described above, by incubating with a mouse anti-human collagen II mAb and a rabbit anti-human actin Ab for 60 minutes at RT. The primary antibodies were revealed with a TRITC conjugated goat anti-rabbit IgG and a FITC conjugated sheep anti-mouse IgG.

Adipogenic differentiation

At passage 4, hASCs were plated at 10^4 hASC/cm^2 and induced to differentiate in adipogenic conditions with a 21-day, scheduled, pulsed induction composed of 48 hours of induction followed by 48 hours of maintenance (see Tab. II). Adipogenic differentiation was confirmed by Oil Red O (2% w/v Oil Red O in 60% isopropanol) lipid droplet staining.

HASC-scaffold constructs

Undifferentiated or osteogenic pre-differentiated hASCs (10^5 cells/scaffold) were seeded on porous (60%) hydroxyapatite blocks (HAP) (kindly provided by Permedica S.p.A., Merate, Italy and Biomaterials Research Center, University of Milan, Italy), human cancellous bone fragments (kindly provided by the Musculoskeletal Tissue Bank, Lombardy Region, Italy) titanium screws (Permedica S.p.A., Merate, Italy) and deproteinized bovine bone granules (Bio-Oss®, 0.25-1 mm, Geistlich Pharma AG, Biomaterials Division, Wolhusen, Switzerland). Cells were allowed to adhere overnight to scaffolds in microcentrifuge tubes and then the scaffolds were transferred to a 24-well plate and cultured under static conditions either in control or osteogenic media (Tab. II). To evaluate calcium depots, Alizarin Red S quantification was performed as described above.

Scanning Electron Microscopy (SEM)

HASCs grown on scaffolds for 14 days were analyzed by SEM. The constructs were fixed in glutaraldehyde (2% in 0.1 M sodium cacodylate buffer) overnight at 4°C, and dehydrated with a series of graded ethanol and examethildisilazane. Samples were mounted on aluminium stubs, sputter-coated with gold/palladium and were examined with a scanning electron microscope (JSM-840A, Jeol Ltd., Tokyo, Japan).

Statistical analysis

Statistical analyses (Student's t-test and Two-way ANOVA) were performed using GraphPad Prism v5.00 (GraphPad Software, San Diego, CA, USA).

RESULTS

Culture and expansion of hASCs

HASCs were derived from 23 liposuction aspirates. Isolated hASCs generally presented a period of quiescence of about one week and then started to rapidly proliferate, showing a homogeneous fibroblast-like shape (Fig.

1a). We isolated an average of 3.5-4x10^5 progenitor cells/mL of raw adipose tissue and the proliferation rate of hASCs was quite stable: in a month of culture we obtained between 10^8 and 10^9 cells from 5X10^5 hASCs; moreover, their proliferation rate and the cellular yield was unaffected by cryopreservation (data not shown). The hASCs growth rate was also maintained by growing cells in medium supplemented with 5% FBS instead of 10%, whereas cells cultured in 1% FBS were quiescent for more than three weeks before showing apoptotic signals (data not shown). The hASCs doubling time ranged between 60 and 90 hours, and under our experimental conditions it depended on the cell plating density and on the time in culture, but we did not observe any correlation with the donor's age. The clonogenic efficiency of hASCs remained constant until passage 4 (Fig.1b): indeed, at the first passage, 13.2± 5.4% hASCs (n=4) were clonogenic and this frequency was maintained to passage 4 (11.67± 2.52%). The hASC colony-forming capacity progressively decreased starting from the fifth passage (7± 2%) until the eighth passage, during which only 3± 2% of all cells appeared to be clonogenic.

Phenotypic profile of hASCs: characterization by FACS analysis

A representative cytofluorimetric analysis of hASCs at passage IV is shown in Figures 1c to 1f. Cells appeared as a homogenous population with a similar size and granularity (Fig. 1c): 99% of hASCs expressed CD13 and 66% of them co-expressed CD105 (Fig. 1d); 68% of hASCs are $CD44^+$ whereas almost 35% expressed CD49d while 28% were $CD44^+$-$CD49d^+$ (Fig. 1e). As expected, hASCs were $CD45^-$ (Fig. 1f). The phenotypic profiles of several hASCs populations were quite similar, as shown in Table III.

Differentiation of Adipose-derived Stem Cells

The multipotency of MSCs isolated from adult subcutaneous adipose tissue was examined by promoting differentiation into chondrogenic, adipogenic and osteogenic lineages (Fig. 2-7).

Chondrogenic and differentiation

HASCs were differentiated into chondrogenic lineage under either monolayer or pellet conditions (micromass). Although it is known that a three-dimensional environ-

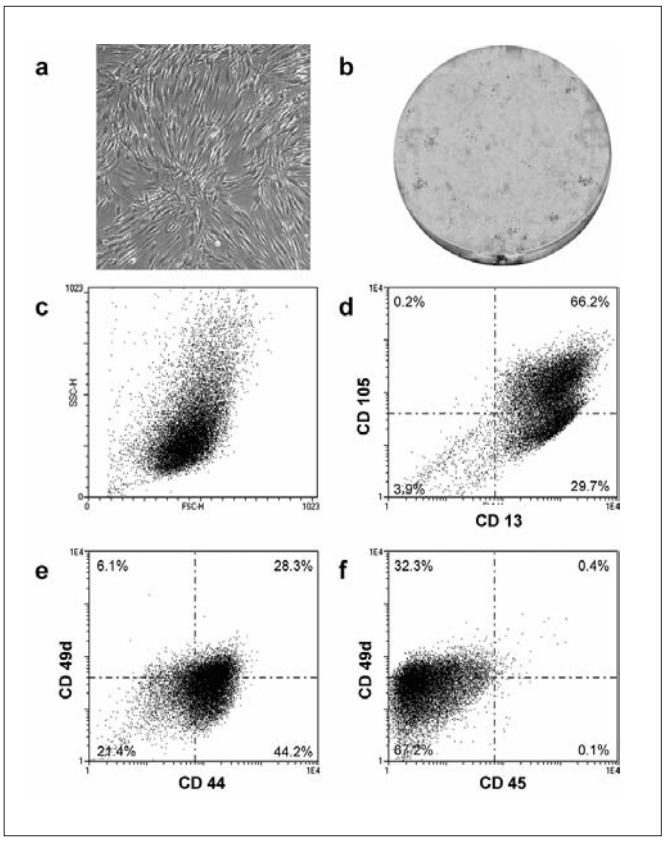

Fig. 1 - *Characterization of hASCs: cell-morphology, CFU-F and co-expression of MSC markers:* ***(a)*** *Fibroblast-like morphology of hASCs by phase contrast microscopy (40X magnification);* ***(b)*** *CFU-F assay of hASC at passage I (dilution 12 cells/cm^2);* ***(c-f)*** *FACS analysis of hASC at passage IV stained with CD13, CD105, CD44, CD49d and CD45 mAb. Size and granularity are depicted* ***(c)****. The numbers in the corners of each panel indicate the % of single- and double-stained cells, gating the populations with specific isotype controls.*

TABLE III - hASCs PHENOTYPIC PROFILE

	% positive cells mean ± SD
CD 90	95.48 ± 5.35
CD 13	94.30 ± 8.36
CD 105	90.43 ± 11.83
CD 29	88.77 ± 20.40
CD 44	87.97 ± 11.43
CD 49d	78.90 ± 20.44
CD 54	77.86 ± 12.51
CD 34	5.51 ± 4.47
CD 14	2.96 ± 3.18
CD 45	2.16 ± 1.89
CD 71	1.52 ± 0.76

Flow cytometry analysis of cultured hASCs at passage IV, isolated from 5 independent donors. Results are expressed as % of positive cells (mean ± SD) gating the population with the isotype controls. Markers are listed from the more to the less positive expression; markers under 5% of expression are to be considered negative.

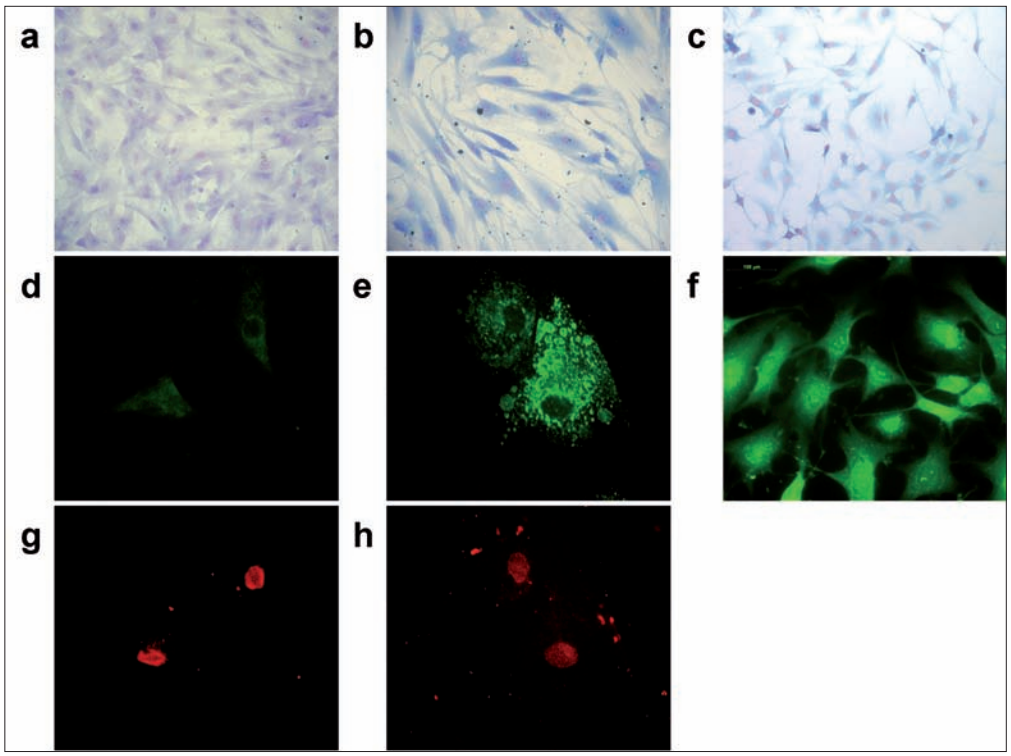

Fig. 2 - *Chondrogenic-differentiated hASCs show glycosaminoglycans production and collagen II expression compared to undifferentiated hASCs:* ***(a-c)*** *glycosaminoglycans staining by Alcian Blue 8GX: monolayer culture of hASCs maintained in control* ***(a)*** *and chondrogenic media* ***(b)*** *magnification). Primary chondrocytes* ***(c)*** *are shown as positive control (100X magnification);* ***(d-h)*** *collagen II expression: immunofluorescence of control* ***(d, g)*** *and chondrogenic differentiated hASCs* ***(e, h)*** *cultured for 21 days (630X magnification) and of primary chondrocytes* ***(f)*** *(400X magnification). Cells are stained with a mouse anti-human collagen II revealed with a sheep α-murine-FITC Ab* ***(d, e)****, and a rabbit anti-human actin Ab revealed with a goat α-rabbit-TRITC Ab* ***(g-h)****.*

ment ameliorates chondrogenic differentiation, hASCs cultured for three weeks in chondrogenic medium in the wells were stained using Alcian blue (Fig. 2b), whereas cells preserved in control medium were just barely stained (Fig. 2a). Primary chondrocytes were also included to confirm the staining specificity (Fig. 2c). The staining deposition was quantified by an image analysis tool: differentiated hASCs contain 30% more glycosaminoglycans than control cells (132.1 and 101.6 AU, respectively; data not shown). Furthermore, to confirm chondrogenic differentiation, type II collagen expression was analyzed by immunofluorescence experiments. As shown in Figures 2e and 2f, only cells cultured for 21 days under chondrogenic conditions and primary chondrocytes expressed type II collagen, whereas no signal is present in undifferentiated hASCs (Fig. 2d). Differentiated hASCs grown in pellet culture for 21 days generated bigger micromasses, as shown in Figures 3a and 3b; the volume of differentiated micromasses were significantly greater than the volumes of the control ones (2.6mm^3 compared to 0.6mm^3; p<.001, n=7), with an average increase of 305%. In addition, control micromasses appeared more fragile due to the lack of extracellular matrix deposition (unpublished observation). In the chondrogenic micromass, external layer nuclei were abundant and cell morphology evoked primary chondrocytes: cells showed an oval- and less fibroblast-like shape, nuclear membrane appeared quite irregular, with some invaginations, and the cytoplasm was more defined (Fig. 3c). Moreover, sections from the chondrogenic micromass were Alcian Blue positive (Fig 3d). The sulfated GAG content was also quantified with the DMMB assay: the chondrogenic differentiated samples contained a significantly greater amount of GAGs (3.53±0.2 µg/pellet; n=7, p<.001) with an average increase of 130% compared to control samples (1.53±0.2 µg/pellet, n=7) (Fig. 4).

Adipogenic differentiation

hASCs differentiated towards adipocyte and produced lipid vacuoles after only one week of differentiation; and their size increased further when cells were cultured in adipogenic conditions. Fourteen-day adipogenic-differentiated hASCs were heavily stained by Oil Red O (Fig. 5b), in contrast to control hASCs, in which no stained vacuoles were detected (Fig. 5a). Quantitative analysis confirmed the observed increase of Oil Red staining in adipogenic-induced hASCs (data not shown).

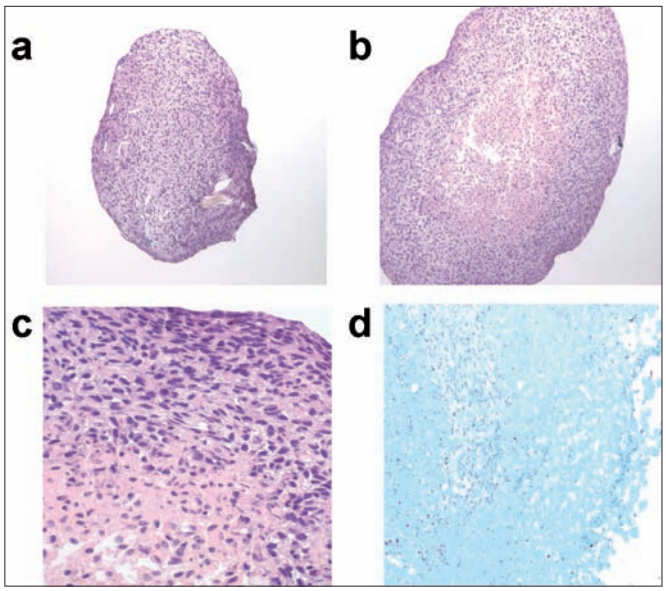

Fig. 3 - *Micromasses of chondrogenic differentiated hASCs show an increase in extracellular matrix production compared to undifferentiated ones:* ***(a-c)*** *microphotographs of sections of hASCs micromasses cultured for 21 days in control* ***(a)*** *and chondrogenic* ***(b)*** *media and stained with Haematoxilin/Eosin (100X magnification);* ***(c)*** *magnification of the section of the chondrogenic pellet (400X magnification);* ***(d)*** *section of a chondrogenic differentiated micromass stained by Alcian Blue 8GX (400X magnification).*

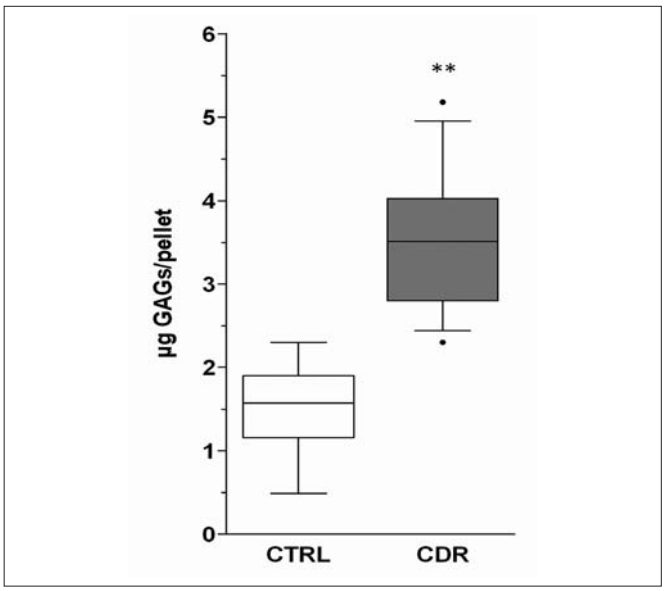

Fig. 4 - *Micromasses of chondrogenic differentiated hASCs show an increase in sulfated GAGs production. Glycosaminoglycans quantification by DMMB assay of control (CTRL) and chondrogenic differentiated (CDR) micromasses expressed as µg GAG content for each pellet. Data are depicted as boxplot: the box represents first quartile, median and third quartile; the whiskers represent the 10-90% of the interval; the dots represent the outliers. Unpaired Student's t-test was performed (**= p< .01).*

Osteogenic differentiation

HASCs were able to differentiate into osteoblast-like cells, as demonstrated by cell-morphology change, calcium deposition, osteopontin expression, and alkaline phosphatase activity. Hematoxylin and eosin staining highlighted morphological differences: undifferentiated hASCs showed a fibroblast-like aspect (Fig. 6a), whereas osteogenic-differentiated hASCs were less outstretched, with a cubical shape (Fig. 6b). Furthermore, hASCS differentiated for 28 days (Fig. 6d) produced abundant mineralized calcium-positive nodules on the cell surface, in contrast to control cells, in which the calcified matrix was almost undetectable (Fig. 6c). The calcified matrix of the osteogenic-differentiated hASCs increased more than three times compared to the control ones (data not shown). To monitor the early hASC osteogenic differentiation process, we looked for the expression of early osteogenic markers such as osteopontin (OPN) and alkaline phosphatase (ALP).

Intracellular OPN expression was induced in 14-day differentiated hASCs (Fig. 6f), whereas it was undetectable in undifferentiated cells (Fig. 6e). Osteosarcoma

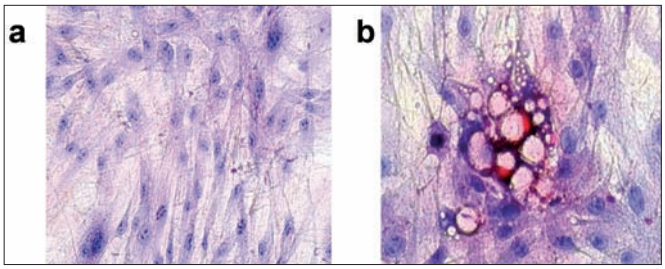

Fig. 5 - *Adipogenic-differentiated hASCs show lipid vacuole formation. hASCs cultured for 14 days in control* ***(a)*** *and adipogenic* ***(b)*** *media (200X magnification): lipid vacuoles are positively stained by Oil Red O and counterstained with hematoxylin.*

SaOs-2 cells were OPN-positive (Fig. 6g). The study of alkaline phosphatase activity (ALP) at different time points (7, 14 and 21 days) in four different hASCs populations cultured in CTRL and osteogenic medium showed that differentiated hASCs produced a significant level of ALP after 14 days of differentiation (between 13% and 37% compared to control cells) (Fig. 7a-d). Moreover, two samples slightly increased their ALP activity (Figs. 7a-b) after only 7 days of differentiation, and a significant, although variable, upregu-

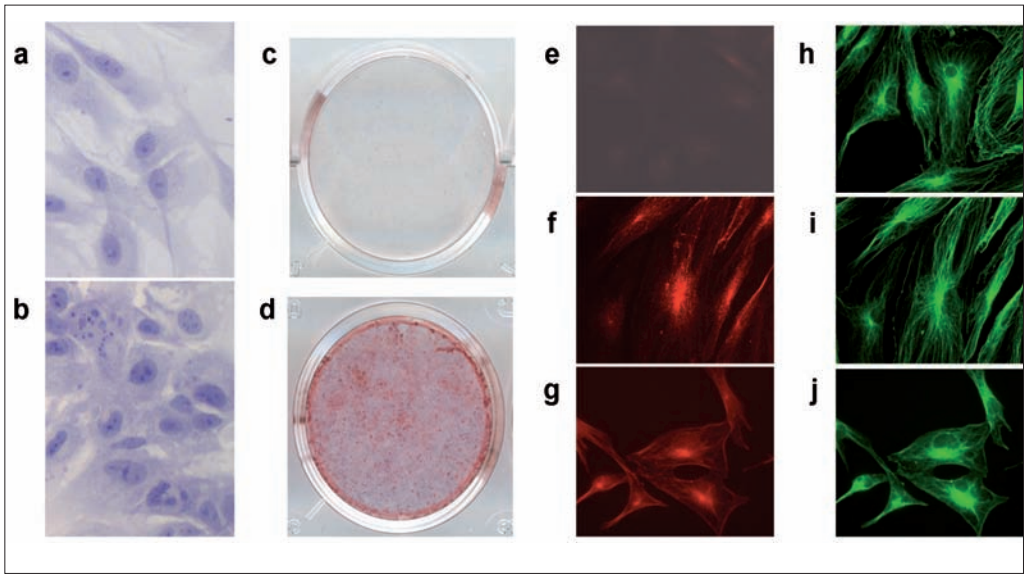

Fig. 6 - *Osteogenic-differentiated hASCs show a different morphology and expression of specific osteogenic markers compared to undifferentiated hASCs:* ***(a-b)*** *morphology of 14-day cultured hASCs in control* ***(a)*** *and osteogenic* ***(b)*** *media (200X magnification);* ***(c-d)*** *Alizarin Red S staining of extracellular calcified matrix of control* ***(c)*** *and osteogenic-differentiated hASCs* ***(d)*** *cultured for 21 days. Osteopontin expression* ***(e-j)****: immunofluorescence of control* ***(e, h)*** *and osteogenic differentiated hASCs* ***(f, i)*** *cultured for 14 days. SaOs-2 cells* ***(g, j)*** *are shown as positive control. Cells are stained with a rabbit anti-human osteopontin Ab revealed with a goat α-rabbit-TRITC Ab* ***(e-g)*** *and a mouse anti-human α-tubulin mAb revealed with a sheep α-murine-FITC Ab* ***(h-j)*** *(400x magnification).*

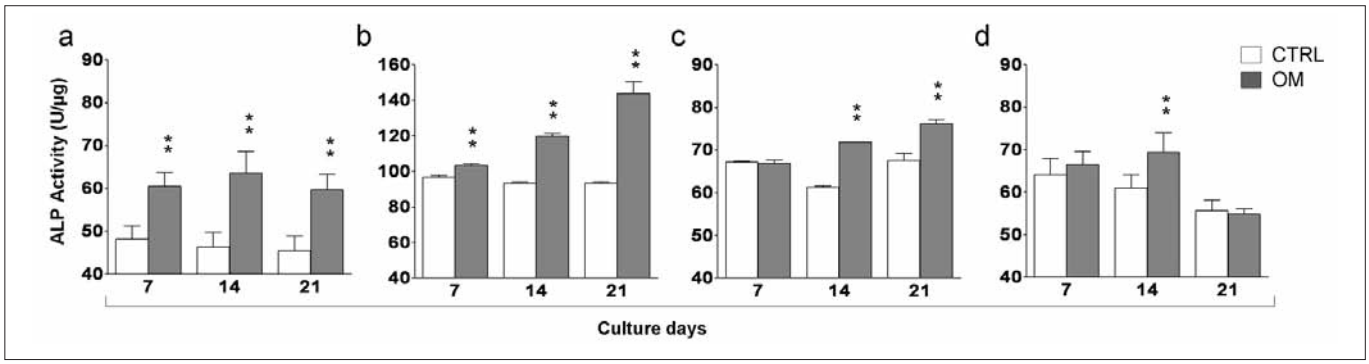

Fig. 7 - *Osteogenic-differentiated hASC show an increase in alkaline phosphatase activity compared to undifferentiated ones. Kinetic study of alkaline phosphatase activity (ALP) of hASCs from four donors* ***(a-d)*** *in control (empty bars) and osteogenic (grey bars) cultured for 7, 14 and 21 days. Each bar represents the mean±SD (n=3 independent experiments for each cell population) of normalized values of ALP units for µg of protein.Two-way ANOVA analysis was also performed: **= p<.01 OM vs CTRL.*

lation was maintained until 21 days in three out of the four samples (Figs. 7a-c). However, in one sample alone, ALP increased after 14 days of differentiation and significantly decreased at day 21 (Fig. 7d). We suggest that the kinetic enzymatic differences observed in our samples may be due to the basal ALP activity of the CTRL cells.

Differentiated hASCs interact with natural and synthetic scaffolds

The ability of hASCs to adhere to scaffolds routinely applied in orthopedics and oral implantology was tested by seeding them on biomaterials such as hydroxyapatite granules (HAP), human cancellous bone fragments, titanium, and deproteinized bovine bone (Bio-Oss®). HASCs cultured for at least two weeks adhered quite well to all the tested scaffolds and they proliferated in the same way as cells maintained in culture wells (polystyrene) (Figs. 8b-f). Moreover, hASCs properly colonized and overwhelmed the surface and pores of all the biomaterials, as shown on HAP (Fig. 8a); no cellular toxicity due to the release of any substances from scaffolds was observed.

Undifferentiated hASCs seeded on HAP, human bone and deproteinized bovine bone fragments were able to produce a greater amount of calcium compared to hASCs grown on polystyrene (Figs. 9a-b, empty bars), indicating that they have their own osteoinductive properties

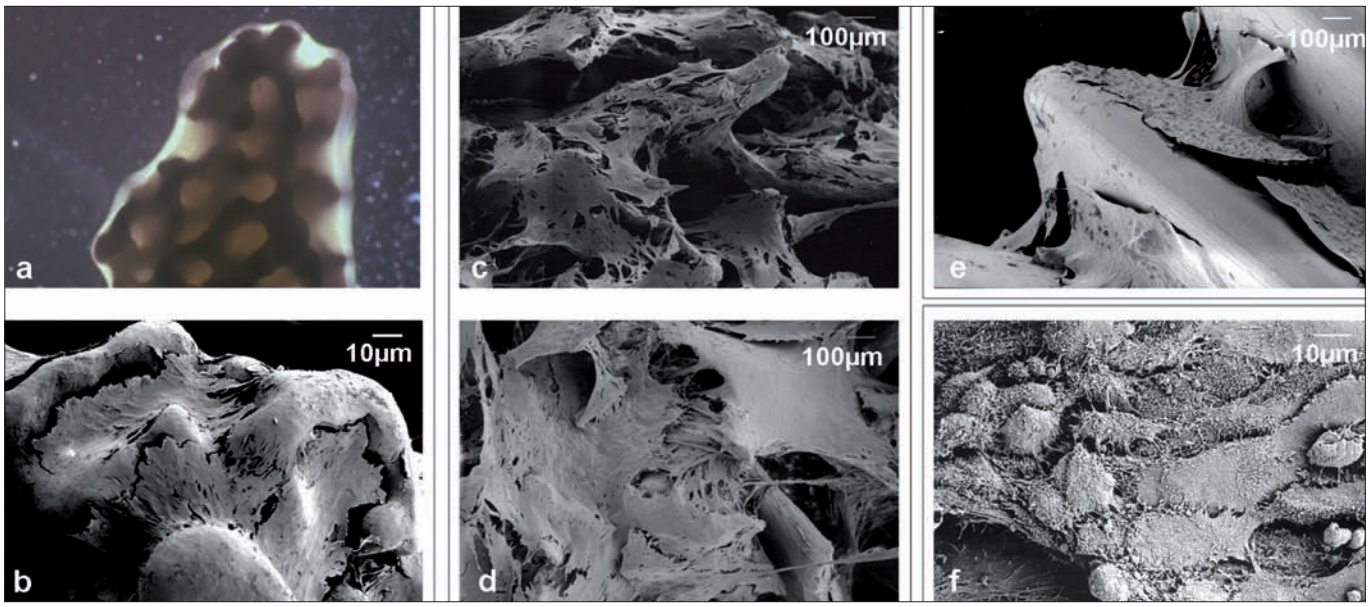

Fig. 8 - *Osteogenic differentiated hASCs seeded on scaffolds display good adhesive properties. HASCs maintained in control and osteogenic media for 14 days on monolayer were seeded for 14 additional days on scaffolds.* ***(a-b)*** *Osteogenic differentiated hASCs on HAP granules: optical microphotograph* ***(a)*** *40X magnification) and* ***(b)*** *SEM picture;* ***(c-d)*** *SEM pictures of control* ***(c)*** *and osteogenic differentiated hASCs* ***(d)*** *seeded on human cancellous bone fragments;* ***(e-f)*** *SEM pictures of osteogenic differentiated hASC seeded on on a titanium screw* ***(e)*** *and on a Bio-Oss® fragment* ***(f)****.*

even in the absence of any specific differentiative biochemical stimuli. In particular, undifferentiated hASCs grown on HAP and human bone for 14 days (Fig. 9a) produced an average increase of 36% and 174%, respectively, compared to undifferentiated cells grown for the same amount of time on polystyrene. The same phenomenon is detectable after five weeks in undifferentiated cells cultured on deproteinized bovine bone (Bio-Oss®): indeed, this scaffold enhanced their calcium deposition by 173% compared to undifferentiated hASCs grown on polystyrene for the same period of time (Fig. 9b).

Cells cultured on monolayer for two weeks in osteogenic medium showed a calcium deposition increase of 29% with respect to undifferentiated hASCs (Fig. 9a); this up-regulation was strongly enhanced for hASCs cultured in osteogenic medium and seeded on scaffold. Indeed, for differentiated cells grown on titanium, we measured an increase of 106% compared to control cells grown on polystyrene, an increase of 138% for differentiated hASCs cultured on HAP, and an increase of 468% for those on human bone fragments (Fig 9a). After 5 weeks of culture, the amount of calcium deposition in differentiated hASCs cultured on monolayer further increased by 95% compared to hASCs cultured in control medium. The amount of calcium produced by differentiated hASCs seeded on HAP was further enhanced: it was 216% greater than control hASCs cultured on polystyrene, and an even more significant increase of 546% was observed in cells seeded on deproteinized bovine bone (Fig. 9b).

DISCUSSION

In the last few years, tissue engineering and regenerative medicine are becoming prominent fields in research and in modern medicine due to the aging population and to the shortage of donor tissues (24, 25). A convenient cellular source for autologous cells will aid the approach of regenerative medicine and we think that mesenchymal stem cells derived from adipose tissue present several advantages compared to BMSC. Indeed, fat is routinely available in large amounts from liposuction and a copious number of MSCs can be isolated from a minimal amount of withdrawn tissue (26, 27), with minimal discomfort for the patient compared to bone marrow aspiration. Moreover, the number of purified progenitor cells is quite abundant (12). Here we report that, independently of the age of the donor, hASCs proliferate quite constantly over an extended period of time while showing clonogenic activity and a stable phenotypic profile, thus confirming data

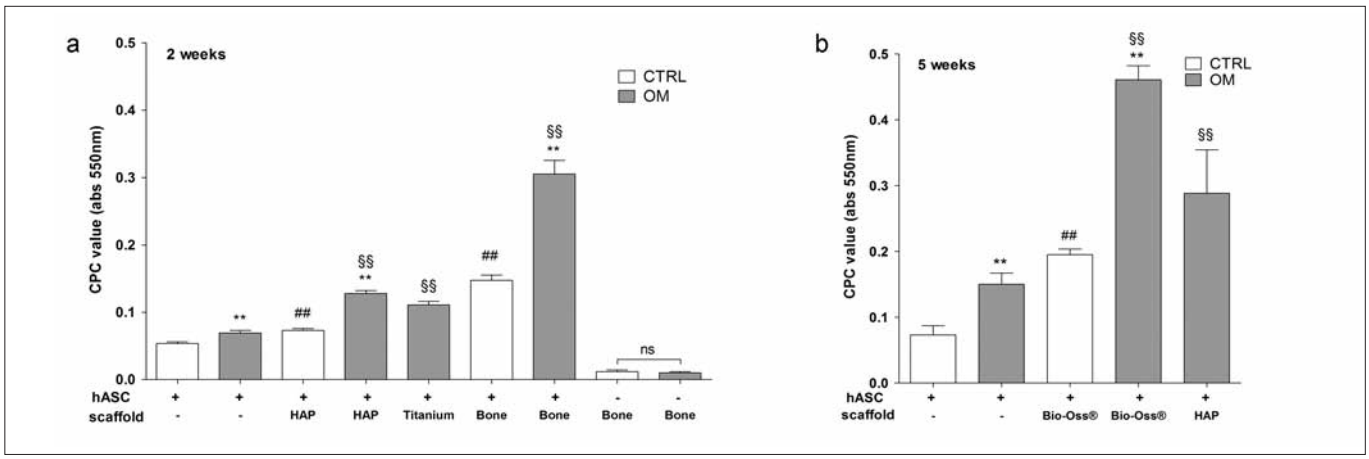

Fig. 9 - *Scaffolds support and promote osteogenic differentiation of hASCs. Extracellular calcified matrix quantification of hASCs cultured in monolayer and in the presence of scaffolds after 2 weeks **(a)** and 5 weeks **(b)**. Each bar is represented as mean ± SD (n=3). One-way ANOVA was also performed: **= p<.01 OM vs CTRL; ## = p<.01 CTRL cells on scaffold vs CTRL cells alone; §§ = p<.01 OM cells on scaffold vs OM cells alone.*

from other laboratories (12, 24, 28, 29). Interestingly enough, and in contrast with the defined mesenchymal stromal cells markers expression (30, 31), in some populations we found a consistent number of hASCs expressing CD34, as also described by others (11, 32). Further studies on the characterization of the CD34+ population are in progress to evaluate if sorted hASC-subpopulations (32, 33) are directed towards a prominent osteospecificity *in vitro*, likely permitting more rapid and efficient future applications.

HASCs differentiated *in vitro* towards chondrocytes and adipocyte-like cells (15, 26, 28, 34). Our data showed that the enhancement of GAG deposition is really due to the chondrogenic differentiation process. Although we showed a significant increase of volume of the chondrogenic micromasses compared to undifferentiated ones, the data on DNA content (not shown) suggested that the increase in volume is only partially due to cell proliferation, and thus it is correlated to a greater GAG-positive matrix production in differentiated samples.

The chondrogenic differentiation of hASCs is not yet well documented in an *in vivo* study, whereas several reports on plastic surgery validate the presence of progenitor cells in fat that do not only fill the damaged adipose tissue, but also reduce fibrotic scar formation due to revascularization (35, 36). The broad potential clinical application of hASCs is also be based on their ability to differentiate towards endothelial (25,37) (unpublished data) and muscle cells (13), making them a promising tool for regeneration of highly vascularized bones and in the cardiovascular field, respectively.

In this study we focused our interest on the osteogenic potential of hASCs, showing that, at the early stage of the differentiation process, ALP activity and osteopontin expression were significantly upregulated, as was the calcified matrix production when the time of differentiation was extended. The observed different ALP activity modulation did not always correlate with the later abundant calcified matrix formation, and we might explain this result by the fact that we did not specifically analyze only the newly synthesized enzyme (GPI-linked ALP fraction), but rather, the whole ALP enzymatic pool. Indeed, we performed preliminary experiments on soluble and GPI-linked ALP fractions isolated from control and osteogenic-induced hASCs; we observed that the GPI-linked compartment derived from differentiated hASCs contained more than double the ALP activity of the same fraction derived from control hASCs, indicating that the enzyme is rapidly upregulated during differentiation (unpublished data). The cellular localization of osteopontin, usually abundant in bone tissue, where it regulates mineralization by acting on bone cell adhesion and the osteoclast function, appears during the differentiation process: we detected OPN expression predominantly in the Golgi and in Endoplasmic Reticulum Compartment, confirming its peculiar secretory pathway (38). However, we also observed an OPN nuclear localization, as described by Junaid et al (39), which could be correlated either with cell division or with an early differentiation state of some hASCs (data not shown).

HASCs were induced to differentiate into osteoblast-like cells both by biochemical stimuli and by the physical interaction with scaffolds. Interestingly enough, the adherence of hASCs to the tested scaffolds induced hASCs to spontaneously differentiate. We are uncertain whether this is due to the chemical features of the scaffolds or more to the 3D structure, which may allow the hASCs to activate specific intracellular pathways that cause extracellular matrix deposition. To address this issue, other types of scaffold need to be analyzed. Moreover, the same number of hASCs loaded on scaffolds and induced to differentiate in osteogenic medium for 15 days were able to produce a more abundant calcified extracellular matrix deposition compared to cells cultured on polystyrene, showing a synergistic effect of the osteogenic medium whose magnitude appeared to depend on the characteristics of the biomaterial, such as chemical properties, porosity, roughness and others. In particular, hydroxyapatite, human bone and deproteinized bovine bone fragments seemed more osteoinductive compared to titanium, despite the fact that hASCs seeded on titanium screws produced levels of calcified matrix significantly greater than those produced by hASCs plated on polystyrene. Human bone fragments appeared to be the most rapid osteogenic inducers for the hASCs, suggesting the use of constructs made with hASCs and bone fragment for the treatment of large bone defects.

We have also shown that the calcium production is time dependent; indeed, the calcified matrix produced by hASCs differentiated on HAP granules significantly increased after five weeks compared to the one formed in two weeks. We observed that hASCs directly differentiated in the presence of the scaffolds, and produced a level of calcified extracellular matrix that was similar to the one produced by cells pre-differentiated on polystyrene and loaded on the scaffold next (unpublished observation). Thus, loading undifferentiated hASCs directly on scaffolds could shorten the time between the adipose tissue removal and the use of differentiated cells, allowing faster clinical application.

In the near future, due to the large number of hASCs and their rapid osteogenic differentiation *in vitro,* it will be feasible to test several types of scaffolds, and to use them to study the effect of additional osteogenic stimulants, like Bone Morphogenetic Proteins (BMPs) and other growth factors, and their combined action. However, we are still at the beginning and many other aspects need to be addressed further, such as the behavior of hASCs seeded on scaffolds and cultured in bioreactors under dynamic conditions, and their osteogenic differentiation capacity in critical osteoarticular defects in animal models (37, 40).

In conclusion, human ASCs may be considered an easily accessible cellular source, and consequently a possible future tool for autologous cell-based regeneration of skeletal defects in orthopedics and oral implantology. Moreover, hASCs may be a convenient cellular model for studying biological differentiation processes and an ideal system for screening drugs which could affect osteogenic progenitor cells and thus skeletal-tissue repair and bone metabolism.

ACKNOWLEDGMENTS

The authors would like to thank Antonina Parafioriti, Donatella Lattuada, Luca C. Rovati, Antonio Bizzozzero and Permedica S.p.A for their precious help.

This study was partially supported by the following grants: FIRST 2005, FIRST 2006 and PRIN 2006 (area 09, prot. 2006091907_003, Italian Ministry of Universities and Research).

Conflict of interest statement
No authors have proprietary interests regarding the present study.

Address for correspondence:
Anna T. Brini
Via Vanvitelli, 32
20129 Milan, Italy
e-mail: anna.brini@unimi.it

REFERENCES

1. Abdallah BM, Kassem M. Human mesenchymal stem cells: from basic biology to clinical applications. Gene Ther 2008; 15: 109-16.
2. Le Blanc K, Ringdén O. Mesenchymal stem cells: properties and role in clinical bone marrow transplantation. Curr Opin Immunol 2006; 18: 586-91.
3. Trombi L, Mattii L, Pacini S, D'Alessandro D, Battolla B, Orciuolo E, Buda G, Fazzi R, Galimberti S, Petrini M. Human autologous plasma-derived clot as a biological scaffold for mesenchymal stem cells in treatment of orthopedic healing. J Orthop Res 2008; 26: 176-83.
4. Savarino L, Baldini N, Greco M, Capitani O, Pinna S, Valentini S, Lombardo B, Esposito MT, Pastore L, Ambrosio L, Battista S, Causa F, Zeppetelli S, Guarino V, Netti PA. The

performance of poly-ε-caprolactone scaffolds in a rabbit femur model with and without autologous stromal cells and BMP4. Biomaterials 2007; 28: 3101-3109.
5. Viateau V, Guillemin G, Bousson V, Oudina K, Hannouche D, Sedel L, Logeart-Avramoglou D, Petite H. Long-bone critical-size defects treated with tissue-engineered grafts: a study on sheep. J Orthop Res 2007; 25: 741-9.
6. Djouad F, Mrugala D, Noel D, Jorgensen C. Engineered mesenchymal stem cells for cartilage repair. Regen Med 2006; 1: 529-37.
7. Ando W, Tateishi K, Hart DA, Katakai D, Tanaka Y, Nakata K, Hashimoto J, Fujie H, Shino K, Yoshikawa H, Nakamura N. Cartilage repair using an in vitro generated scaffold-free tissue-engineered construct derived from porcine synovial mesenchymal stem cells. Biomaterials 2007; 28: 5462-70.
8. Bosch P, Musgrave DS, Lee JY, Cummins J, Shuler T, Ghivizzani TC, Evans T, Robbins TD Huard,. Osteoprogenitor cells within skeletal muscle. J Orthop Res 2000; 18: 933-44.
9. Sakaguchi Y, Sekiya I, Yagishita K, Muneta T. Comparison of human stem cells derived from various mesenchymal tissues: superiority of synovium as a cell source. Arthritis Rheum 2005; 52: 2521-9.
10. Nöth U, Osyczka AM, Tuli R, Hickok NJ, Danielson KG, Tuan RS. Multilineage mesenchymal differentiation potential of human trabecular bone-derived cells. J Orthop Res 2002; 20: 1060-9.
11. Zuk PA, Zhu M, Mizuno H, Huang J, Futrell JW, Katz AJ, Benhaim P, Lorenz HP, Hedrick MH. Multilineage cells from human adipose tissue: implications for cell-based therapies. Tissue Eng 2001; 7: 211-28.
12. De Ugarte DA, Morizono K, Elbarbary A, et al. Comparison of multi-lineage cells from human adipose tissue and bone marrow. Cells Tissues Organs 2003; 174: 101-9.
13. Mizuno H, Zuk PA, Zhu M H. Lorenz HP, Benhaim P, Hedrick MH.. Myogenic differentiation by human processed lipoaspirate cells. Plast Reconstr Surg 2002; 109: 199-211.
14. Guilak F, Lott KE, Awad HA Cao Q, Hicok KC, Fermor B, Gimble JM. Clonal analysis of the differentiation potential of human adipose-derived adult stem cells. J Cell Physiol 2006; 206: 229-37.
15. Gimble JM, Katz AJ, Bunnell BA. Adipose-derived stem cells for regenerative medicine. Circ Res 2007; 100: 1249-60.
16. Helder MN, Knippenberg M, Klein-Nulend J, Wuisman PI. Stem cells from adipose tissue allow challenging new concepts for regenerative medicine. Tissue Eng 2007; 13: 1799-1808.
17. Gimble J, Guilak F. Adipose-derived adult stem cells: isolation, characterization, and differentiation potential. Cytotherapy 2003; 5: 362-9.
18. D'Ippolito G, Schiller PC, Ricordi C, Roos BA, Howard GA. Age-related osteogenic potential of mesenchymal stromal stem cells from human vertebral bone marrow. J Bone Miner Res 1999; 14: 1115-22.
19. Quarto R, Thomas D, Liang CT. Bone progenitor cell deficits and the age-associated decline in bone repair capacity. Calcif Tissue Int 1995; 56:123-9.
20. Castro-Malaspina H, Gay RE, Resnick G, Kapoor N, Meyers P, Chiarieri D, McKenzie S, Broxmeyer HE, Moore MA. Characterization of human bone marrow fibroblast colony-forming cells (CFU-F) and their progeny. Blood 1980; 56: 289-301.
21. Bodo M, Lilli C, Bellucci C, Carinci P, Calvitti M, Pezzetti F, Stabellini G, Bellocchio S, Balducci C, Carinci F, Baroni T. Basic fibroblast growth factor autocrine loop controls human osteosarcoma phenotyping and differentiation. Mol Med 2002; 8: 393-404.
22. Halvorsen YD, Franklin D, Bond AL, Hitt DC, Auchter C, Boskey AL, Paschalis EP, Wilkison WO, Gimble JM. Extracellular matrix mineralization and osteoblast gene expression by human adipose tissue-derived stromal cells. Tissue Eng 2001; 7: 729-41.
23. Barbosa I, Garcia S, Barbier-Chassefière V, Caruelle JP, Martelly I, Papy-García D. Improved and simple micro assay for sulfated glycosaminoglycans quantification in biological extracts and its use in skin and muscle tissue studies. Glycobiology 2003; 13: 647-53.
24. Fraser JK, Wulur I, Alfonso Z, Hedrick MH. 2006. Fat tissue: an underappreciated source of stem cells for biotechnology. Trends Biotechnol 24: 150-4.
25. Zannettino AC, Paton S, Arthur A, Khor F, Itescu S, Gimble JM, Gronthos S. Multipotential human adipose-derived stromal stem cells exhibit a perivascular phenotype in vitro and in vivo. J Cell Physiol 2007; 214: 413-21.
26. Awad HA, Wickham MQ, Leddy HA, Gimble JM, Guilak F. Chondrogenic differentiation of adipose-derived adult stem cells in agarose, alginate, and gelatin scaffolds. Biomaterials 2004; 25: 3211-22.
27. Choi YS, Cha SM, Lee YY, Kwon SW, Park CJ, Kim M. Adipogenic differentiation of adipose tissue derived adult stem cells in nude mouse. Biochem Biophys Res Commun 2006; 345: 631-7.
28. de Girolamo L, Sartori MF, Albisetti W, Brini AT. Osteogenic differentiation of human adipose-derived stem cells: comparison of two different inductive media. J Tissue Eng Regen Med 2007; 1: 154-7.
29. Lee RH, Kim B, Choi I, Kim H, Choi HS, Suh K, Bae YC, Jung JS. Characterization and expression analysis of mesenchymal stem cells from human bone marrow and adipose tissue. Cell Physiol Biochem 2004; 14: 311-24.
30. Baksh D, Song L, Tuan RS. Adult mesenchymal stem cells: characterization, differentiation, and application in cell and gene therapy. J Cell Mol Med 2004; 8: 301-16.
31. Reyes M, Verfaillie CM. Characterization of multipotent adult progenitor cells, a subpopulation of mesenchymal stem cells. Ann NY Acad Sci 2001; 938: 231-5.
32. Sengenes C, Miranville A, Maumus M, de Barros S, Busse

R, Bouloumie A. Chemotaxis and differentiation of human adipose tissue CD34+/CD31-progenitor cells: role of SDF-1 released by adipose tissue capillary endothelial cells. Stem Cells 2007; 25: 2269-76.
33. Yamamoto N, Akamatsu H, Hasegawa S, Yamada T, Nakata S, Ohkuma M, Miyachi E, Marunouchi T, Matsunaga K. Isolation of multipotent stem cells from mouse adipose tissue. J Dermatol Sci 2007; 48: 43-52.
34. Schmitt B, Ringe J, Haupl T, Notter M, Manz R, Burmester GR, Sittinger M, Kaps C. 2003. BMP2 initiates chondrogenic lineage development of adult human mesenchymal stem cells in high-density culture. Differentiation 71: 567-77.
35. Rigotti G, Marchi A, Galiè M, Baroni G, Benati D, Krampera M, Pasini A, Sbarbati A. Clinical treatment of radiotherapy tissue damage by lipoaspirate transplant: a healing process mediated by adipose-derived adult stem cells. Plast Reconstr Surg 2007; 119: 1409-24.
36. Coleman SR. Structural fat grafting: more than a permanent filler. Plast Reconstr Surg 2006; 118 (Suppl): S108-20.
37. Scherberich A, Galli R, Jaquiery C, Farhadi J, Martin I. Three-dimensional perfusion culture of human adipose tissue-derived endothelial and osteoblastic progenitors generates osteogenic constructs with intrinsic vascularization capacity. Stem Cells 2007; 25: 1823-9.
38. Denhardt DT, Noda M. Osteopontin expression and function: role in bone remodelling. J Cell Biochem 1998; 30-31 (Suppl): S92-102.
39. Junaid A, Moon M, Harding G, Zahradka P. Osteopontin localizes to the nucleus of 293 cells and associates with polo-like kinase 1. Am J Physiol Cell Physiol 2006; 292: C919-26.
40. Fini M, Giardino R. In vitro and in vivo tests for the biological evaluation of candidate orthopedic materials: Benefits and limits. Journal of Applied Biomaterials & Biomechanics 2003; 1: 155- 63.